Qualitative Analysis of Signaling Networks Using Petri Nets and Invariant Computation

Rza Bashirov *

Posted Date: 5 February 2026

doi: 10.20944/preprints202602.0388.v1

Keywords: petri net; qualitative modeling; place invariant; transition invariant; signaling pathway; melanoma

 doi:10.20944/preprints202602.0388.v1

Article

Qualitative Analysis of Signaling Networks Using Petri Nets and Invariant Computation

Rza Bashirov

Department of Mathematics, Faculty of Arts and Sciences, Eastern Mediterranean University, Famagusta 99628 North Cyprus, Mersin-10, Türkiye; rza.bashirov@emu.edu.tr; Tel.: +90-392-630-10-05

Abstract

Qualitative analysis of biochemical reaction systems reveals fundamental system-level properties that are independent of precise kinetic parameters, often context-dependent, or experimentally inaccessible. By focusing on structural and topological features — such as conservation relations, feedback loops, and pathway interconnections — qualitative analysis identifies invariant behaviors, robustness mechanisms, and potential failure modes inherent to the signaling network. In this study, we use Petri nets as a formal modeling framework to conduct qualitative analysis of the integrated MAPK and PI3K/Akt signaling network. By exploiting structural properties including place invariants, transition invariants, and siphons, the analysis establishes a direct correspondence between the Petri net structure and biologically meaningful conservation laws, signaling modules, and characteristic dynamic behaviors. The results demonstrate that the proposed model is structurally consistent, biologically plausible, and modular. Minimal semi-positive place invariants confirm mass conservation, indicating that proteins and enzymes circulate within closed molecular pools. Minimal semi-positive transition invariants identify canonical kinase–phosphatase cycles underlying sustained and reversible signaling. Hierarchical decomposition reveals a modular organization reducible to reusable enzymatic motifs, reflecting biological reuse across cascades and supporting scalability. Additionally, the identification of sixteen siphons that are also traps highlights persistent subsystems that ensure continuous regulator availability, confirming the robustness and dynamic sustainability of the integrated network.

Keywords: petri net; qualitative modeling; place invariant; transition invariant; signaling pathway; melanoma

1. Introduction

Structural properties of signaling networks are as critical to cancer therapy as the behavior of individual molecular components. Accordingly, the investigation of features such as decomposition, modularity, feedback motifs, and invariant subnetworks within the integrated mitogen-activated protein kinase (MAPK) and phosphatidylinositol 3-kinase/protein kinase B (PI3K/Akt) signaling network is essential for understanding melanoma progression and therapeutic failure. In melanoma, constitutive activation of MAPK signaling is prevalent; however, its pharmacological inhibition frequently results in rapid drug resistance mediated by compensatory activation of the PI3K/Akt pathway. This phenomenon cannot be adequately explained by isolated mutations or single pathway elements. Rather, it emerges from the modular organization of the signaling network, which enables survival-associated modules to remain operative even when proliferation-driven modules are effectively suppressed.

Structural analysis offers a systems-level rationale for this robustness and clarifies why single-pathway targeting strategies often prove insufficient in melanoma treatment. By decomposing the network into functional modules and identifying structurally conserved cores alongside fragile inter-modular interfaces, it becomes possible to discriminate between subnetworks that sustain persistent survival signaling and those that are susceptible to coordinated disruption. These insights are fundamental to the rational design of combination therapies, as they indicate which modules must be

 doi:10.20944/preprints202602.0388.v1

simultaneously targeted to prevent adaptive network rewiring. Importantly, an emphasis on structural properties permits robust conclusions even in the absence of detailed kinetic parameters, rendering this approach particularly suitable for addressing the intrinsic heterogeneity and complexity of melanoma cancer.

Each biological system — whether a signaling, a metabolic, or a gene regulatory — can be formally represented as a collection of interacting biochemical reactions. Petri nets provide a natural and rigorous modeling formalism for such systems: molecular species are mapped to places, biochemical reactions to transitions, and the stoichiometric relationships between reactants and products to directed arcs. Owing to this close structural correspondence, Petri nets are particularly well suited for capturing both the organization and the dynamics of biochemical reaction networks.

The application of Petri nets in systems biology dates back to the early 1990s, following the work of Reddy and colleagues, who first recognized the strong analogy between the behavior of biochemical reaction systems and the underlying execution semantics of Petri nets [1]. Since then, Petri nets have been extensively adopted for modeling and analyzing biochemical networks, as illustrated by a broad body of works encompassing continuous, hybrid, colored, hierarchical, stochastic, and fuzzy Petri net extensions, and provide numerous case studies that highlight its analytical power [2–9].

Several prior works have specifically addressed MAPK and PI3K/Akt signaling using Petri net–based approaches. For instance, in [10], a continuous Petri net model explicitly incorporates crosstalk between the MAPK and PI3K/Akt pathways via Ras, identifying Ras and its regulatory machinery as potential therapeutic targets for overcoming BRAF inhibitor resistance in melanoma. In [11], siphon analysis in Petri nets combined with graph-theoretic centrality measures was proposed as a strategy for identifying targets for multi-component therapies within the MAPK pathway. Furthermore, the practical utility of place and transition invariants (P- and T-invariants) for revealing modular organization in biochemical networks, including MAPK signaling, has been systematically established in the work of Heiner and co-workers [12]. In particular, they reported how invariant-based analysis can be used to decompose large and complex biochemical networks into biologically meaningful modules.

Building on these methodological foundations, the present study employs the Snoopy software [13] to construct a Petri net model of the integrated MAPK and PI3K/Akt signaling network, and the Charlie software [14] to compute and analyze structural properties, including P-invariants, T-invariants, as well as siphons and traps. The originality of our approach lies in the fact that, to the best of our knowledge, this is the first study to systematically investigate the integrated MAPK and PI3K/Akt signaling network — of central importance for understanding melanoma and other cancer types — from the perspective of decomposition, modularity, and other structural properties using invariant-based Petri net analysis.

This study shows that the proposed model is structurally consistent, biologically meaningful, and modular. Minimal semi-positive P-invariants confirm conservation of all major signaling components across their biochemical states, indicating that proteins and enzymes circulate within closed molecular pools. Minimal semi-positive T-invariants identify canonical kinase–phosphatase cycles that support sustained and reversible signaling in both pathways. Hierarchical decomposition reveals a modular organization in which the complex network can be reduced to reusable enzymatic motifs, reflecting biological reuse across signaling cascades and supporting model scalability and interpretability. The identification of sixteen siphons that also function as traps provides further evidence of robustness, as these persistent subsystems ensure continuous availability of key regulators, including Ras, RAF, MEK, ERK, Akt, and their associated phosphatases. Together, the invariant and siphon analyses demonstrate that the integrated MAPK and PI3K/Akt network is mass-preserving, dynamically sustained, and inherently robust. Overall, the invariant-based Petri net analysis offers a concise, kinetics-independent framework for validating signaling models, revealing modular structure, and supporting subsequent quantitative simulations, perturbation analyses, and exploration of therapeutic strategies targeting MAPK–PI3K/Akt crosstalk.

 doi:10.20944/preprints202602.0388.v1

The reminder of the paper is organized as follows. Section 2 presents the biological context and Section 3 outlines the research methodology adopted in this work. Section 4 details modularity in biochemical reaction networks and simulation results are presented and analyzed, together with a detailed discussion of the structural and behavioral properties of the network, including minimal semi-positive P-invariants and T-invariants and their biological interpretation in Section 5. The paper concludes with Section 6, a summary of the main findings and perspectives for future research.

2. Biological Context

This section summarizes the MAPK and PI3K/Akt signaling pathways and their molecular interconnections, based on information from Kyoto encyclopedia of genes and genomes (KEGG) [15,16], Reactome, a database of reactions, pathways and biological processes, [17], and relevant literature.

2.1. MAPK Pathway

The MAPK pathway represents a canonical multi-stage signal transduction cascade in which external stimuli are propagated through a sequence of activation and deactivation events. Signal transmission proceeds through a hierarchical chain of components, where each stage activates the next via phosphorylation, forming a directed and layered structure.

Activation is initiated at membrane-associated receptors and transmitted through an intermediate switching element (Ras), followed by a cascade RAF–MEK–ERK. This architecture exhibits typical features of computational pipelines, including amplification, modularity, and separation of concerns between upstream signal detection and downstream response execution.

Regulatory control is implemented through dedicated deactivation processes mediated by phosphatases, which ensure bounded signal duration, reversibility, and prevention of uncontrolled propagation. These opposing activation–deactivation cycles naturally form conserved substructures that are well suited for invariant-based analysis.

2.2. PI3K/Akt Pathway

The PI3K/Akt pathway constitutes a parallel signaling module that processes the same upstream inputs but emphasizes persistence and stability of the system state. Signal propagation is mediated through the production of an intermediate membrane-associated state variable (PIP3), which enables conditional activation of downstream components. Activation of the central effector (Akt) requires multiple coordinated events, reflecting logical conjunctions frequently encountered in formal models. Negative regulation is achieved through a dedicated counteracting process (PTEN), which restores the system to its baseline state and enforces resource conservation. From a modeling perspective, this pathway is characterized by state-dependent transitions, feedback control, and competition between activating and deactivating processes.

2.3. Interrelationship Between MAPK and PI3K/Akt Pathways

The MAPK and PI3K/Akt pathways form a coupled network rather than independent linear chains. They share common upstream activators and exhibit bidirectional regulatory interactions at downstream levels. These interconnections introduce non-trivial dependencies, feedback loops, and conditional constraints that significantly influence global system behavior. Cross-regulation between pathways can either reinforce or suppress signal propagation, depending on system state, thereby preventing dominance of a single pathway and enhancing robustness. Shared regulatory components, particularly phosphatases, operate across pathway boundaries and contribute to coordination and synchronization of signaling activity.

From a computational perspective, the integrated MAPK–PI3K/Akt network exemplifies a distributed, resource-constrained system with concurrency, feedback, and modular organization. These characteristics motivate the use of formal modeling frameworks, such as Petri nets, to analyze con-

 doi:10.20944/preprints202602.0388.v1

servation relations, invariant structures, and emergent qualitative behavior independent of kinetic parameters.

Figure 1 schematically depicts the MAPK and PI3K/Akt pathways and their crosstalk, explicitly identifying key kinases and phosphatases such as RasGTP, RAFP, MEKPP, PTEN, and PP2A, while additional regulatory processes are represented by Phase 1 through Phase 6.

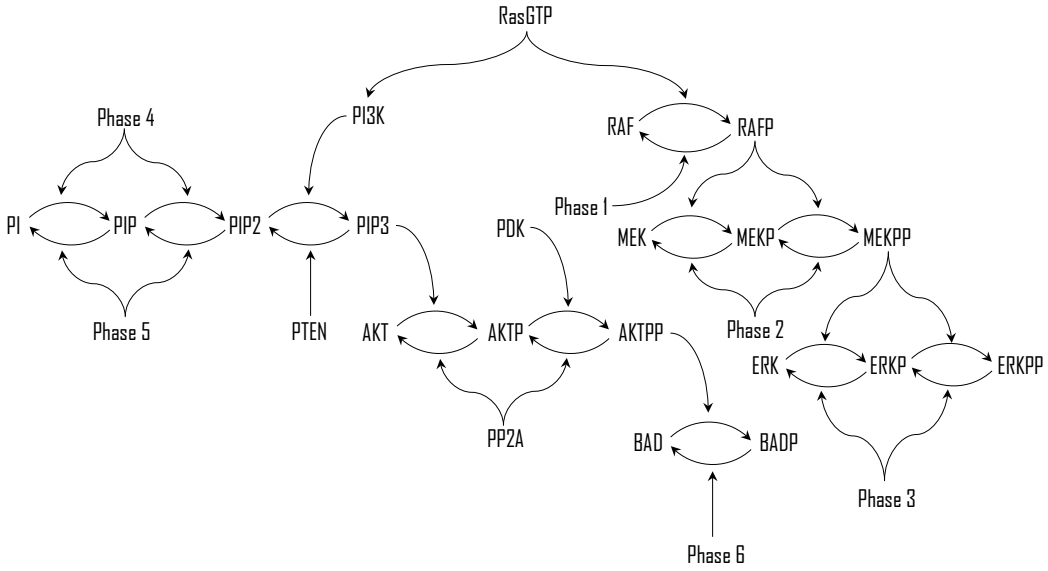

Figure 1. Schematic illustration of cascade of reactions in MAPK and PI3K/Akt pathways and their crosstalk.

3. Research Method

This study adopts a structural Petri net–based methodology to analyze signaling networks at an abstract, qualitative level. We focus on well-established Petri net properties that capture conservation, connectivity, and deadlock-related behavior, independently of kinetic parameters. For further details, the reader is directed to [18], a timeless and foundational paper on the principles of Petri nets.

Definition 1. *A Petri net is a 5-tuple* $R = (P, T, I, O, M_0)$ *such as*

- $P = \{p_1, \ldots, p_n\}$ *is the set of places;*
- $T = \{t_1, \ldots, t_m\}$ *is the set of transitions;*
- $I \subseteq P \times T$ *is the set of input arcs;*
- $O \subseteq T \times P$ *is the set of output arcs;*
- $M_0 : P \to \mathbb{N}$ *is the initial marking.*

The only rule one has to know about Petri nets is the rule for transition firing. Although the rule seems to be very simple, its implication in Petri net theory is very deep and complex. In the following, we elaborate on the regulations that govern the token flow game associated with Petri nets.

A transition t is said to be *enabled* or *enable* if each input place p is marked with at least $w(p,t)$ tokens. Thus, t is enabled if $M(p) \geq w(p,t)$ holds for all $p \in {}^\bullet t$ where $w(p,t)$ and ${}^\bullet t$ are, respectively, the weight of the arc from p to t and the set of t's input places. A transition t is said to be *disabled* or *disable* in marking M if there exists an input place p with the number of tokens less than $w(p,t)$. That is, t is disabled if there exists $p \in {}^\bullet t$ such that $M(p) < w(p,t)$ holds. An enabled transition may or may not *fire* or *occur* depending on whether or not the event actually takes place. Occurrence of an enabled transition t removes $w(p,t)$ tokens from $p \in {}^\bullet t$, and adds $w(t,p)$ tokens to $p \in t^\bullet$, where $w(t,p)$ is the

 doi:10.20944/preprints202602.0388.v1

weight of the arc from t to p and $t^\bullet$ stands for the set of t's output places. Stated more mathematically, occurrence of enabled transition t changes the state of the Petri net from M to $M^{'}$ as follows:

$$M^{'}(p) = M(p) - w(p,t) + w(t,p), \forall p \in P.$$

A *self-loop* (or simple loop) is a bidirectional connection between a place and a transition. A Petri net is *pure* if no such loops exist, ensuring that places are not simultaneously consumed and produced by the same transition. In modeling terms, purity enforces an explicit separation between consumption and production mechanisms. A Petri net is *ordinary* if all arc weights are equal to one, corresponding to unit stoichiometry. A Petri net is *homogeneous* if all outgoing arcs of a place have identical multiplicities, implying uniform consumption rates across transitions. Structural *connectedness* ensures that all nodes belong to a single component, while *strong connectedness* guarantees mutual reachability via directed paths.

Additional structural constraints are used to assess balance and competition. A Petri net has *non-blocking multiplicity* if outgoing arc weights of each place do not exceed incoming ones, reflecting balanced production and consumption. A Petri net is *conservative* if every transition preserves the total token count, indicating structural conservation laws. A Petri net is *static conflict-free* if no place feeds multiple transitions, thereby eliminating structural competition for resources. We also consider the absence of specific structural elements. Petri nets with no input transitions ensure that every transition requires at least one pre-place, while no output transitions imply that every transition produces tokens. Similarly, the absence of input places ensures that every place is produced by at least one transition, and the absence of output places guarantees that every place is eventually consumed. These properties exclude spontaneous creation, pure degradation, and unbounded accumulation.

Deadlock-related behavior is analyzed using *siphons* and *traps*. A siphon is a non-empty set of places that, once emptied, cannot be refilled; a trap is a non-empty set of places that, once marked, cannot lose all tokens. Formally, a set of places S is a siphon if ${}^\bullet S \subseteq S^\bullet$, and a set T is a trap if $T^\bullet \subseteq {}^\bullet T$. The *siphon–trap property* states that in a live Petri net, every siphon contains a marked trap, ensuring that siphons cannot be completely emptied. This property is central to verifying liveness and robustness in large-scale Petri net models.

The qualitative analysis in this work is based on *P-invariants* and *T-invariants*. Let A denote the incidence matrix of a Petri net. A non-trivial, non-negative integer solution x of $A \cdot x = 0$ is a P-invariant, while a solution y of $A^T \cdot y = 0$ is a T-invariant. P-invariants characterize conserved weighted sums of places and imply boundedness, whereas T-invariants represent transition sequences that leave the marking unchanged.

Computationally, invariant analysis reduces to solving homogeneous linear systems over the non-negative integers. This analysis supports model validation by revealing structural conservation laws and cyclic execution patterns. P-invariants with identical supports are linearly dependent, and non-negative linear combinations of invariants remain invariants.

All Petri net models in this study were constructed using Snoopy, and invariant analysis was performed using Charlie, enabling systematic verification of structural correctness and consistency.

4. Modularity of Reaction Networks

4.1. Basic Modular Patterns

Biological reaction networks exhibit an inherent modular structure, whereby complex cellular behaviors arise from the interconnection of simple and recurrent reaction patterns. These patterns, referred to as reaction modules, can be identified at multiple levels of organization and provide a natural foundation for both biological interpretation and Petri net–based modeling. In systems biology, modularity supports scalability, robustness, and the reuse of functional components across different cellular contexts.

 doi:10.20944/preprints202602.0388.v1

We consider reaction modules ranging from elementary transformations to enzymatic cycles under explicit kinetic assumptions. Each module constitutes a reusable building block that can be embedded into larger biochemical networks while preserving its structural and functional characteristics.

At the most elementary level, an irreversible reaction $A \to B$ represents a fundamental transformation pattern. It captures unidirectional processes such as synthesis or degradation and establishes directionality within reaction networks. Despite its simplicity, this pattern serves as a core building block for more complex reaction structures.

Extending this pattern to a reversible reaction $A \rightleftharpoons B$ models equilibrium-driven processes that are ubiquitous in metabolic and signaling networks. Reversibility introduces bidirectionality and buffering capacity, enabling dynamic balance between molecular species. In hierarchical representations, the forward and backward reactions can be abstracted into a single reversible module, illustrating how multiple elementary steps can be grouped into a coherent functional unit.

Enzymatic catalysis is captured by reactions of the form $A + E \to B + E$, typically interpreted under Michaelis–Menten kinetics. This module represents enzyme-mediated conversion through substrate binding and product release, explicitly encoding enzyme specificity and conservation. It replaces a simple reaction with a more biologically realistic, yet still modular, abstraction.

This concept is further extended to reversible enzymatic reactions $A + E \rightleftharpoons B + E$, together with their hierarchical abstractions. At a detailed level, both directions are mediated by enzyme–substrate complexes, whereas at a higher level the entire process is represented as a compact reversible module. This illustrates how enzymatic detail can be selectively exposed or hidden depending on the abstraction level required.

Under mass-action kinetics, enzymatic reactions are explicitly modeled as $A + E \rightleftharpoons AE \to B + E$, making all elementary steps and enzyme conservation across free and bound states explicit. This reinforces the modular interpretation of enzyme-driven processes.

Finally, cyclic enzymatic modules arise from coupled reversible reactions such as $A + E1 \rightleftharpoons AE1 \to B + E1$ and $B + E2 \rightleftharpoons BE2 \to A + E2$. These cycles represent closed catalytic processes involving distinct enzymes for forward and backward transformations. While detailed representations expose multiple binding and conversion steps, hierarchical abstractions condense the cycle into a single functional module that captures its net reversible behavior. Such cycles are characteristic of metabolic pathways and naturally give rise to invariant-based structural properties.

In summary, biochemicCharal reaction networks are inherently modular and hierarchical. Elementary reactions, reversible transformations, enzymatic mechanisms, and enzymatic cycles can each be treated as self-contained, reusable modules. Hierarchical representations enable abstraction without loss of essential functionality, supporting qualitative analysis, invariant-based reasoning, and scalable modeling of large biochemical systems.

4.2. Petri Net Model of the Integrated MAPK-PI3K/Akt Network

Figure 2 presents the Petri net model of the integrated MAPK and PI3K/Akt signaling pathways, constructed using the Snoopy tool. The resulting Petri net consists of 50 places and 67 transitions. Hierarchical modeling is supported through macro transitions, depicted as concentric squares, which are used to abstract reversible reactions. Read arcs, shown as pairs of opposing arcs, impose enabling conditions on transition firing without modifying token counts.

Structural inspection shows that the MAPK and PI3K/Akt pathways are composed of five and six hierarchical cyclic enzymatic modules, respectively. Each module represents a pair of coupled reversible enzymatic reactions of the form $A + E1 \rightleftharpoons AE1 \to B + E1$ and $B + E2 \rightleftharpoons BE2 \to A + E2$, Consequently, the integrated network contains a total of eleven such hierarchical cyclic modules.

Each cyclic module can be further decomposed into two reversible enzymatic reaction modules, yielding an overall decomposition into twenty-two enzymatic reaction units. This hierarchical refinement can be applied recursively until the network is reduced to its elementary reaction motifs. Depending on the underlying biochemical mechanisms, this process ultimately terminates in either the simple irreversible reaction pattern $A \to B$ or the canonical enzymatic reaction pattern $A + E \to B + E$.

Preprints.org (www.preprints.org) | NOT PEER-REVIEWED | Posted: 5 February 2026 doi:10.20944/preprints202602.0388.v1

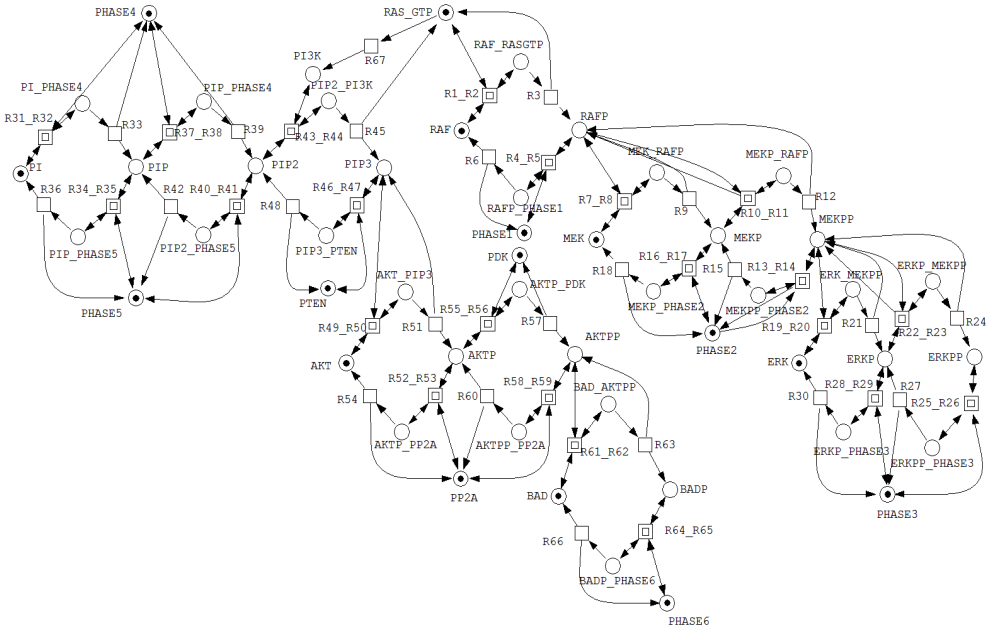

Figure 2. Hierarchical representation of the Petri net model of the integrated MAPK–PI3K/Akt signaling network, imported from Snoopy software.

5. Simulations and Qualitative Analysis

Qualitative analysis of the integrated MAPK–PI3K/Akt Petri net model was performed using the Charlie software [14]. The analysis efficiently verified key structural and behavioral properties of the model, providing formal evidence that the network architecture is suitable for studying signaling robustness and adaptive behavior characteristic of melanoma.

5.1. Structural Properties

The analysis confirms that the Petri net is pure and loop-free, excluding read and double arcs. This property enforces an explicit separation between production and consumption events, which is essential for accurately modeling sequential signal transduction steps involved in melanoma-driving MAPK and PI3K/Akt signaling.

All arcs have unit weight, indicating that the model is an ordinary Petri net. In addition, identical weights on all outgoing arcs of each place establish homogeneity. From a modeling perspective, this ensures uniform token flow across competing reactions, enabling fair representation of alternative signaling routes that become relevant in melanoma under targeted pathway inhibition.

The Petri net is both connected and strongly connected, implying that all signaling components are mutually reachable through reaction sequences. This structural property formally captures pathway cross-talk and feedback, which are known to facilitate compensatory activation of PI3K/Akt signaling in melanoma following MAPK pathway suppression. The satisfaction of the non-blocking multiplicity property further guarantees balanced token flow, preventing structural deadlocks and supporting sustained signal propagation.

The net is non-conservative, reflecting association and dissociation reactions among signaling components. This is a necessary modeling feature for representing transient complexes and pathway reconfiguration events associated with melanoma progression and drug resistance. The presence of static conflicts indicates shared reactants among alternative transitions, structurally encoding competition between signaling routes—a key mechanism underlying adaptive resistance in melanoma cells.

All transitions have pre-places, satisfying the no-input-transitions property, and all places have pre-transitions, ensuring that signaling components are neither spontaneously created nor independent of upstream reactions. Finally, the no-output-places property guarantees that components cannot

 doi:10.20944/preprints202602.0388.v1

be structurally exhausted, allowing persistent signaling activity. Collectively, these properties support the use of the model for analyzing long-term melanoma signaling behavior under therapeutic perturbations.

5.2. Behavioral Properties

Behavioral analysis shows that the Petri net is 1-bounded (safe) and, more generally, k-bounded, ensuring that token counts remain finite for all places. From a modeling perspective, this guarantees numerical stability of the state space and enables reliable simulation of melanoma signaling dynamics without unbounded accumulation of signaling activity.

The Petri net is live, indicating that every transition can eventually fire and may do so infinitely often. This property formally captures the persistent activation potential of MAPK and PI3K/Akt signaling in melanoma, even under inhibitory perturbations. The net is also reversible, meaning that the system can return to its initial marking through an appropriate firing sequence, reflecting the capacity of melanoma signaling networks to re-establish active states following transient suppression.

The net is not dynamically conflict-free, indicating the presence of competing transitions that cannot be simultaneously enabled. Structurally, this encodes mutually exclusive signaling events and conditional reaction availability. In the context of melanoma, such conflicts correspond to adaptive pathway selection mechanisms that contribute to therapy resistance. Importantly, no dead markings were identified, and the absence of dead transitions ensures that signaling activity cannot become permanently blocked, supporting continuous pathway reactivation.

The Petri net is covered by transition invariants, demonstrating that all reactions participate in cyclic firing sequences capable of reproducing the initial marking. This invariant structure provides formal evidence for sustained signaling loops that underlie long-term melanoma cell survival. Coverage by place invariants further ensures bounded token circulation within each component state space, confirming structural conservation of signaling resources across the integrated MAPK and PI3K/Akt network.

Finally, the net is not strongly connected with respect to transition invariants, indicating the presence of localized cyclic subnetworks. These short reaction cycles structurally represent minimal feedback motifs that enable rapid compensatory responses, a key contributor to the robustness and therapy resistance observed in melanoma signaling systems.

5.3. Minimal Semi-Positive P- and T-Invariants and Their Biological Interpretation

Invariant analysis identified twelve minimal semi-positive P-invariants, each representing a closed set of places whose total token count is preserved. Structurally, each P-invariant aggregates all reachable states of a single signaling entity, establishing conservation laws over its state space. The full set of P-invariants is reported in Table 1.

For example, invariant X_5 includes all places associated with Akt, AktP, AktPP, and their corresponding complexes, indicating that the total Akt concentration remains conserved despite transitions among multiple biochemical states. Similarly, invariant X_8 groups RAF, RAFP, and their associated complexes, reflecting conservation of RAF throughout phosphorylation–dephosphorylation processes. Figures 3–5 illustrate representative net structures corresponding to P-invariants X_1, X_5, and X_8, respectively. All three P-invariants were automatically identified using the Charlie software, after which their biological meanings were interpreted.

These invariants demonstrate that all core components of the integrated MAPK and PI3K/Akt network circulate among multiple functional states without net creation or loss. Consequently, the Petri net is fully covered by place invariants, confirming mass preservation and ensuring physical consistency of the model. This property guarantees that signaling activity is redistributed rather than amplified or depleted, a prerequisite for analyzing long-term network behavior under perturbations.

 doi:10.20944/preprints202602.0388.v1

Table 1. Minimal semi-positive P-invariants and their biological meaning.

Minimal semi-positive P-invariant	Biological meaning
X_1=(PI_PHASE4, PIP_PHASE4, PHASE4)	States of PHASE4
X_2=(PIP_PHASE5, PIP2_PHASE5, PHASE5)	States of PHASE5
X_3=(PI, PIP, PIP2, PIP3, PIP_PHASE5, PIP2_PHASE5, PIP3_PTEN, PI_PHASE4, PIP_PHASE4, PIP2_PI3K, Akt_PIP3)	States of PI
X_4=(AktP_PP2A, AktPP_PP2A, PP2A)	States of PP2A
X_5=(Akt, Akt_PIP3, AktP, AktP_PP2A, AktP_PDK, AktPP, AktPP_PP2A, BAD_AktPP)	States of Akt
X_6=(BAD, BAD_AktPP, BADP, BADP_PHASE6)	States of BAD
X_7=(Ras_GTP, PIP2_PI3K, PI3K, RAF_Ras_GTP)	States of Ras_GTP
X_8=(RAF_RasGTP, RAF, RAFP, RAFP_PHASE1, MEK_RAFP, MEKP_RAFP)	States of RAF
X_9=(MEKP_PHASE2, PHASE2, MEKPP_PHASE2)	States of PHASE2
X_{10}=(MEK_RAFP, MEK, MEKP, MEKPP, MEKP_RAFP, MEKP_PHASE2, MEKPP_PHASE2, ERK_MEKPP, ERKP_MEKPP)	States of MEK
X_{11}=(ERKP_PHASE3, ERKPP_PHASE3, PHASE3)	States of PHASE3
X_{12}=(ERK, ERK_MEKPP, ERKP, ERKPP, ERKP_MEKPP, ERKP_PHASE3, ERKPP_PHASE3)	States of ERK

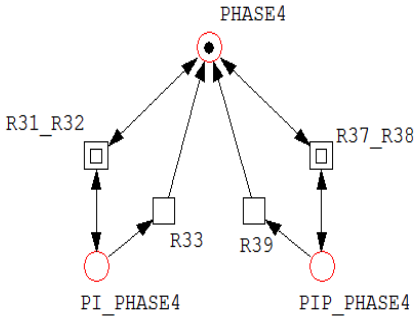

Figure 3. A net fragment illustrating P-invariant X_1 that determines the states of PHASE4.

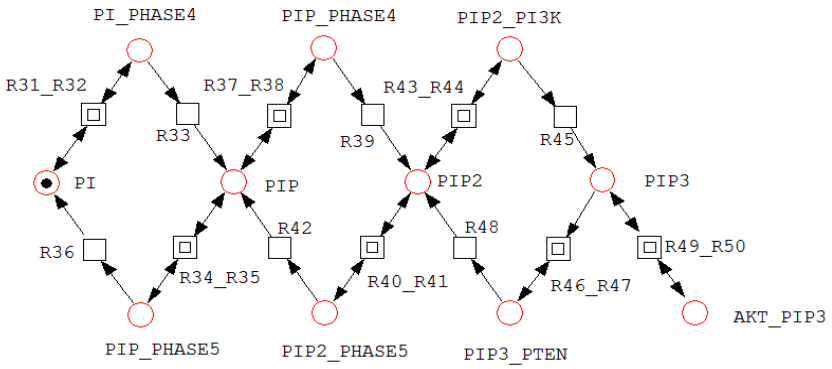

Figure 4. A net fragment illustrating P-invariant X_3 that determines the states of PI.

In addition, eleven minimal semi-positive T-invariants were identified, each corresponding to a minimal cyclic firing sequence of transitions. From a formal perspective, these T-invariants define elementary reaction loops that return the system to its initial marking. Such cycles constitute the basic dynamic building blocks of the network and confirm that all transitions participate in sustained activity. The complete set of T-invariants and their associated transition sequences is summarized in Table 2.

 doi:10.20944/preprints202602.0388.v1

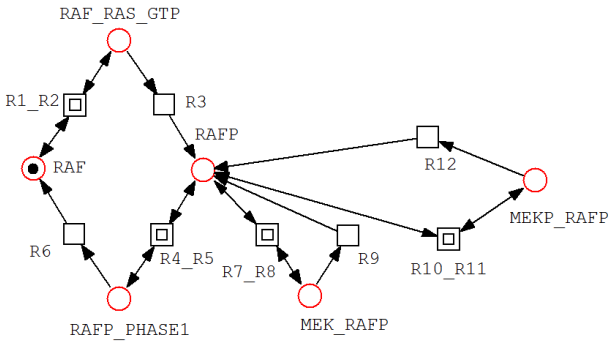

Figure 5. A net fragment illustrating P-invariant X_8 that determines the states of RAF.

Table 2. Minimal semi-positive T-invariants and their biological meaning.

Minimal semi-positive T-invariants	**Biological interpretation**
Y_1=(R33,R36,R31,R34)	Binding of PHASE4 to PI, phosphorylation of PI to PIP and its release, binding of PHASE5 to PIP and dephosphorylation of PIP and its release reactions.
Y_2=(R39, R42, R37, R40)	Binding of PHASE4 to PIP, phosphorylation of PIP to PIP2 and its release, binding of PHASE5 to PIP2 and dephosphorylation of PIP2 and its release reactions.
Y_3=(R45, R48, R43, R46, R67)	Activation of PI3K, binding of PI3K to PIP2, phosphorylation of PIP2 to PIP3 and its release, binding of PTEN to PIP3 and dephosphorylation of PIP3 and its release reactions.
Y_4=(R51, R54, R49, R52)	Binding of PIP3 to Akt, phosphorylation of Akt to AktP and its release, binding of PP2A to AktP and dephosphorylation of AktP and its release reactions.
Y_5=(R57, R60, R55, R58)	Binding of PDK to AktP, phosphorylation of AktP to AktPP and its release, binding of PP2A to AktPP and dephosphorylation of AktPP and its release reactions.
Y_6=(R63, R66, R61, R64)	Binding of AktPP to BAD, phosphorylation of BAD to BADP and its release, binding of PHASE6 to BADP and dephosphorylation of BADP and its release reactions.
Y_7=(R3, R6, R1, R4)	Binding of Ras_GTP to RAF, phosphorylation of RAF to RAFP and its release, binding of PHASE1 to RAFP, dephosphorylation of RAFP and its release reactions.
Y_8=(R9, R18, R7, R16)	Binding of RAFP to MEK, phosphorylation of MEK to MEKP and its release, binding of PHASE2 to MEKP and dephosphorylation of MEKP and its release reactions.
Y_9=(R12, R15, R10, R13)	Binding of RAFP to MEKP, phosphorylation of MEKP to MEKPP and its release, binding of PHASE2 to MEKPP and dephosphorylation of MEKPP and its release reactions.
Y_{10}=(R21, R30, R19, R28)	Binding of MEKPP to ERK, phosphorylation of ERK to ERKP and its release, binding of PHASE3 to ERKP and dephosphorylation of ERKP and its release reactions.
Y_{11}=(R24, R27, R22, R25)	Binding of MEKPP to ERKP, phosphorylation of ERKP to ERKPP and its release, binding of PHASE3 to ERKPP and dephosphorylation of ERKPP and its release reactions.

The coexistence of P- and T-invariant coverage establishes that the Petri net exhibits both conservation and persistent dynamics. Each signaling module is characterized by a conserved state space (P-invariant) and an associated cyclic execution pattern (T-invariant), reflecting a modular organization

 doi:10.20944/preprints202602.0388.v1

based on recurring reaction motifs. This structure enables indefinite operation of individual modules and supports recovery of signaling activity following transient disruptions.

Furthermore, siphon analysis revealed that all siphons are also traps. Formally, this implies that once tokens enter these sets of places, they cannot be completely removed by any firing sequence. Such trap structures guarantee the persistence of specific subnetworks and prevent global deadlock. The identified siphons, listed below, therefore represent invariant subsystems whose activity cannot be structurally extinguished.

Taken together, the invariant and siphon analyses demonstrate that the integrated MAPK and PI3K/Akt Petri net is conservative, dynamically sustained, and modular. Persistent cyclic behavior is structurally enforced, and critical subnetworks remain active under all reachable markings. These properties provide a formal explanation for the robustness of signaling dynamics observed in simulations and motivate the use of the model for studying stable and adaptive behavior in oncogenic signaling networks.

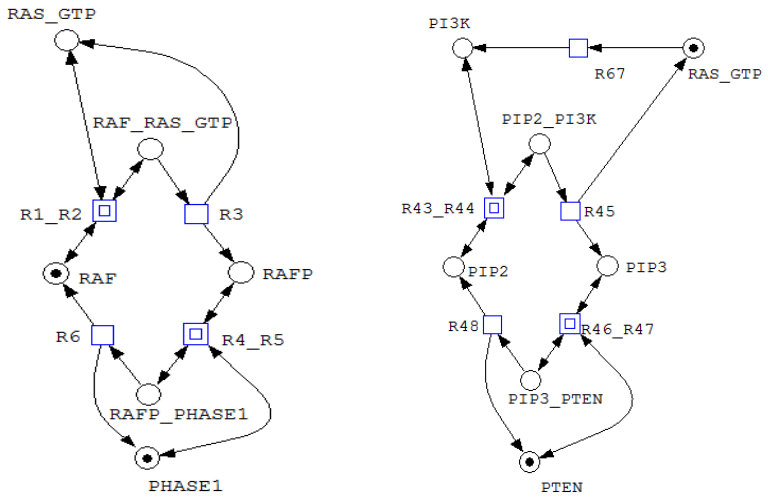

Figure 6. A net fragment illustrating T-invariants Y_7 (in the left) and Y_3 (in the right).

The coexistence of P- and T-invariant coverage establishes that the Petri net exhibits both conservation and persistent dynamics. Each signaling module is characterized by a conserved state space (P-invariant) and an associated cyclic execution pattern (T-invariant), reflecting a modular organization based on recurring reaction motifs. This structure enables indefinite operation of individual modules and supports recovery of signaling activity following transient disruptions.

Furthermore, siphon analysis shows that all identified siphons are also traps. Formally, this means that once tokens enter these place sets, they cannot be completely removed by any admissible firing sequence. Such siphon–trap structures guarantee the persistence of specific subnetworks and exclude global deadlock. Consequently, the siphons listed below define invariant subsystems whose activity cannot be structurally eliminated during execution.

1. S_1=(PI, PIP, PIP2, PIP3, PIP_PHASE5, PIP2_PHASE5, PIP3_PTEN, PI_PHASE4, PIP_PHASE4, PIP2_PI3K, AKT_PIP3)
2. S_2=(AKTP_PP2A, AKTPP_PP2A, PP2A)
3. S_3=(MEK_RAFP, MEK, MEKP, MEKPP, MEKP_RAFP, MEKP_PHASE2, MEKPP_PHASE2, ERK_MEKPP, ERKP_MEKPP)
4. S_4=(AKT, AKT_PIP3, AKTP, AKTP_PP2A, AKTP_PDK, AKTPP, AKTPP_PP2A, BAD_AKTPP)
5. S_5=(PI_PHASE4, PIP_PHASE4, PHASE4)
6. S_6=(BADP_PHASE6, PHASE6)
7. S_7=(BAD, BAD_AKTPP, BADP, BADP_PHASE6)
8. S_8=(RAF_RASGTP, RAF, RAFP, RAFP_PHASE1, MEK_RAFP, MEKP_RAFP)

 doi:10.20944/preprints202602.0388.v1

9. S_9=(ERKP_PHASE3, ERKPP_PHASE3, PHASE3)
10. S_{10}=(RAS_GTP, PIP2_PI3K, PI3K, RAF_RASGTP)
11. S_{11}=(RAFP_PHASE1, PHASE1)
12. S_{12}=(MEKP_PHASE2, PHASE2, MEKPP_PHASE2)
13. S_{13}=(ERK, ERK_MEKPP, ERKP, ERKPP, ERKP_MEKPP, ERKP_PHASE3, ERKPP_PHASE3)
14. S_{14}=(AKTP_PDK, PDK)
15. S_{15}=(PIP_PHASE5, PIP2_PHASE5, PHASE5)
16. S_{16}=(PIP3_PTEN, PTEN)

Taken together, the invariant and siphon analyses demonstrate that the integrated MAPK–PI3K/Akt network is conservative, dynamically sustained, and modular. Persistent cyclic behavior is structurally enforced, and critical signaling subsystems remain active under all reachable markings. These properties provide a formal explanation for the robustness observed in simulation results and are consistent with the well-documented ability of melanoma cells to maintain signaling activity despite targeted therapeutic interventions. Below, selected siphons are interpreted with respect to their functional roles.

Lipid signaling and the PI3K/PTEN module

Siphon S_1 represents the complete phosphoinositide pool together with enzyme-bound intermediates. Its siphon–trap character ensures that lipid-mediated signaling states cannot be structurally exhausted, thereby preserving Akt recruitment and downstream signaling capacity. Siphon S_{15} captures the PHASE5-mediated PIP/PIP2 dephosphorylation loop, indicating persistent regulation of lipid turnover. Siphon S_{16} corresponds to the PTEN–PIP3 subsystem, structurally enforcing the continued presence of negative regulation within PI3K/Akt signaling. Together, these siphons reflect a balanced yet persistent lipid signaling architecture, a feature frequently implicated in melanoma drug resistance.

Akt signaling and survival control

Siphon S_2 contains PP2A and its complexes with phosphorylated Akt, ensuring that Akt deactivation mechanisms cannot be depleted. Siphon S_4 spans all Akt states and associated complexes, confirming that Akt signaling competence is structurally preserved. Siphon S_{14} captures PDK and its interaction with AktP, guaranteeing persistence of full Akt activation. Finally, siphons S_6 and S_7 encompass BAD and its phosphorylated forms together with PHASE6, ensuring sustained control over apoptosis-related signaling. Collectively, these siphons structurally encode survival signaling persistence, a key contributor to therapy resistance in melanoma.

MAPK cascade: RAF–MEK–ERK core

Siphon S_8 represents the RAF module, including RasGTP-dependent activation and phosphatase-mediated inactivation, ensuring that MAPK pathway entry remains structurally available. Siphon S_{10} captures RasGTP and its immediate downstream interactions, reflecting the permanence of the shared upstream activator for both MAPK and PI3K/Akt pathways. Siphons S_3 and S_{12} correspond to the MEK module and its regulatory phosphatase, guaranteeing uninterrupted signal propagation through MEK. Siphons S_{13} and S_9 represent the ERK pool and its associated phosphatase, structurally enforcing both sustained MAPK output and reversibility of ERK activation. These properties are consistent with the rapid pathway reactivation observed in melanoma following MAPK-targeted inhibition.

Overall, siphons S_1–S_{16} closely align with the minimal P-invariants identified earlier, each corresponding to a conserved signaling entity or regulatory module. Their dual siphon–trap nature indicates that the integrated MAPK–PI3K/Akt network is structurally protected against depletion of critical components. This guarantees long-term operability of kinase–phosphatase cycles, robust pathway cross-talk, and persistent adaptive signaling behavior, even in the absence of explicit kinetic assumptions.

 doi:10.20944/preprints202602.0388.v1

6. Conclusions

This work presents Petri net model of an integrated MAPK-PI3K/Akt signaling network and its comprehensive qualitative analysis in terms of P-invariants, T-invariants, siphon-trap property, and other structured characteristics. The results demonstrate that the proposed Petri net model is structurally consistent, modular, and biologically plausible. Minimal semi-positive P-invariants establish strict conservation laws over all major signaling components, formally confirming that proteins and enzymes are neither created nor destroyed but circulate among well-defined biochemical states. Minimal semi-positive T-invariants identify canonical kinase–phosphatase cycles, ensuring sustained and reversible signaling dynamics across both pathways.

The hierarchical decomposition of the network reveals a modular organization in which complex signaling behavior emerges from the composition of reusable enzymatic motifs. From a modeling perspective, this modularity supports scalability, interpretability, and systematic refinement of large signaling networks. From a disease-oriented viewpoint, it reflects the reuse of conserved signaling mechanisms that melanoma cells exploit to maintain pathway activity under pharmacological perturbation.

The identification of sixteen siphons that are simultaneously traps provides strong formal evidence of structural robustness. These siphon–trap structures correspond to signaling subsystems that cannot be depleted by network dynamics, guaranteeing persistent availability of key regulators such as Ras, RAF, MEK, ERK, Akt, and their associated phosphatases. In the context of melanoma, this structural persistence offers an explanation for the resilience of MAPK and PI3K/Akt signaling observed in simulations and is consistent with the emergence of adaptive and compensatory responses following targeted inhibition.

Taken together, the invariant and siphon analyses show that the integrated MAPK and PI3K/Akt network is mass-preserving, dynamically sustained, and resistant to structural shutdown. These properties provide a formal, kinetics-independent explanation for long-term signaling activity and pathway reactivation, phenomena that are closely associated with drug resistance in melanoma.

Overall, the invariant-based Petri net framework employed in this study offers a rigorous approach for validating signaling models, uncovering conserved structure, and reasoning about long-term system behavior without reliance on parameterized kinetics. The results establish a solid foundation for subsequent quantitative simulations, systematic perturbation studies, and the formal analysis of therapeutic strategies aimed at disrupting MAPK–PI3K/Akt pathway crosstalk in melanoma.

Supplementary Materials: Supplementary material related to this article can be found online at https://zenodo.org/records/18467372 and DOI:10.5281/zenodo.18467372.

Data Availability Statement: The original contributions presented in this study are included in the article/Supplementary Material. Further inquiries can be directed to the corresponding author.

References

1. Reddy, V.N.; Mavrovouniotis, M.L.; Liebman, M.N. Petri net representations in metabolic pathways. In Proceedings of the International Conference on Intelligent Systems in Molecular Biology, vol. 1, Bethesda, MD, USA, 6-9 June 1993, pp. 328-–336.
2. Assaf, G.; Liu, F.; Heiner, M. Incremental modelling and analysis of biological systems with fuzzy hybrid Petri nets. *Brief. bioinform.* **2025** *26*(1), bbaf029.
3. Assaf, G.; Liu, F.; Heiner, M.; Herajy, M. Addressing data uncertainty of Caulobacter crescentus cell cycles using hybrid Petri nets with fuzzy kinetics. *Comput. Biol. Medicine* **2025** *186*, 109624.
4. Liu, F.; Heiner, M.; Gilbert, D. Coloured Petri nets for multilevel, multiscale and multidimensional modelling of biological systems. *Brief Bioinform* **2019** *20*(3), 877-–886.
5. Akçay, İ.N.; Bashirov, R. Comparison of modelling approaches demonstrated for p16–mediated signalling pathway in higher eukaryotes. *BioSyst.* **2021** *210*, 104562.
6. Akgün, G.; Bashirov, R. Optimal paradigms for quantitative modeling in systems biology demonstrated for spinal motor neuron synthesis. *Appl. Sci.* **2024** *14*, 10696.

7. Bashirov, R. Modeling disease-drug networks with Petri nets. In Proceedings of the 5th International Conference on Problems of Cybernetics and Informatics, Baku, Azerbaijan, 28–30 August 2023, pp. 1–5.
8. Bashirov, R.; Mehraei, M. Identifying targets for gene therapy of β-globin disorders using quantitative modeling approach. *Inform. Sciences* **2017** *397–398*, 37–47.
9. Bashirov, R. *Petri Nets in Systems Biology: Methodology and Applications*, 1st ed.; Springer Nature: Cham, Switzerland, 2026; (*in press*).
10. Russo, G.; Pennisi, M.; Boscarino, R.; Pappalardo, F. Continuous Petri Nets and microRNA analysis in melanoma. *IEEE/ACM Trans Comput Biol Bioinform.* **2018** *15*(5), 1492–1499.
11. Behinaein, B,; Rudie, K.; Sangrar, W. Petri Net siphon analysis and graph theoretic measures for identifying combination therapies in cancer. *IEEE/ACM Trans. Comput. Biol. Bioinform.* **2016** *15*(1), 231–243.
12. Heiner, M.; Gilbert, D.; Donaldson, R. Petri nets for systems and synthetic biology. In International School on Formal Methods for the Design of Computer, Communication and Software Systems; Bernardo, M., Degano, P., Zavattaro, G. Eds; LNCS 5016; Springer: Heidelberg, Germany, 2008; pp. 215–264.
13. Heiner, M.; Herajy, M.; Liu, F.; Rohr, C. Snoopy a unifying Petri net tool. In Proceeding of the 33rd International Conference on Application and Theory of Petri Nets, Hamburg, Germany, 25-29 June 2012, pp. 398–407.
14. Heiner, M.; Schwarick, M.; Wegener, J.T. Charlie – An extensible Petri net analysis tool. In Proceedings of the 36th International Conference on Application and Theory of Petri Nets and Concurrency, Brussels, Belgium, 21-26 June 2015, pp. 200-–211.
15. Kanehisa, M,; Goto, S. KEGG: kyoto encyclopedia of genes and genomes. *Nucleic Acids Res.* **2000** *28*(1), 27—30.
16. Kanehisa, M.; Goto, S.; Kawashima, S.; Okuno, Y.; Hattori, M. The KEGG resource for deciphering the genome. *Nucleic Acids Res.* **2008** *32*(1), D277–D280.
17. Croft, D.; OḰelly, G.; Wu, G.; Haw, R.; Gillespie, M.; Matthews, L.; Caudy, M.; Garapati, P.; Gopinath, G.; Jassal, B.; et al. Reactome: a database of reactions, pathways and biological processes. *Nucleic Acids Res.* **2011** *39*, D691–D697.
18. Murata, T. Petri nets: properties, analysis and applications. *Proc. of IEEE* **1989** *77*(4), 541–580.
19. Castellano, E.; Downward, J. RAS interaction with PI3K: more than just another effector pathway. *SAGE Journals* **2011** *2*(3), 261–274.
20. Faes, S.; Formond, O. PI3K and AKT: Unfaithful partners in cancer. *Int. J. Mol. Sci.* **2015** *16*(9), 21138–21152.
21. Malek, M.; Kielkowska, A.; Chessa, T.; Clark, J.; Hawkins, P.T.; Stephens, L.R. PTEN regulates PI(3,4)P2 signalling downstream of class I PI3K, *Mol. Cell* **2017** *68*(3), 566–588.
22. Osaki, M., Oshimura, M., Ito, H. PI3K-AKT pathway: its functions and alterations in human cancer. *Apoptosis* **2004** *9*(6), 667–676. Russo, G.; Pennisi, M.; Boscarino, R.; Pappalardo, F. Modeling PI3K/PDK1/Akt and MAPK signaling pathways using continuous Petri nets. In Proceedings of the 13th International Conference on Intelligent Computing Theories and Applications, Liverpool, UK, 7-10 August 2017, pp. 169-–176.